Universiteit Antwerpen

This item is the archived peer-reviewed author-version of:

Head shape disparity impacts pollutant accumulation in European eel

**Reference:**
De Meyer Jens, Belpaire Claude, Boeckx Pascal, Bervoets Lieven, Covaci Adrian, Govindan Malarvannan, De Kegel Barbara, Adriaens Dominique.- Head shape disparity impacts pollutant accumulation in European eel
Environmental pollution - ISSN 0269-7491 - 240(2018), p. 378-386
Full text (Publisher's DOI): https://doi.org/10.1016/J.ENVPOL.2018.04.128
To cite this reference: https://hdl.handle.net/10067/1513420151162165141

uantwerpen.be
Institutional repository IRUA

**Title: Head shape disparity impacts pollutant accumulation in European eel**

*Jens, De Meyer [1], Claude, Belpaire [2], Pascal, Boeckx [3], Lieven, Bervoets [4], Adrian, Covaci [5], Govindan, Malarvannan [5], Barbara, De Kegel [1] & Dominique, Adriaens [1]*

[1] Evolutionary Morphology of Vertebrates, Ghent University, K.L. Ledeganckstraat 35, 9000 Ghent, Belgium; E-mail: jendmeye.demeyer@ugent.be; Barbara.dekegel@ugent.be; Dominique.adriaens@ugent.be

[2] Research Institute for Nature and Forest Research (INBO), Dwersbos 28, 1630 Linkebeek, Belgium; E-mail: claude.belpaire@inbo.be

[3] Isotope Bioscience Laboratory – ISOFYS, Ghent University, Coupure Links 635, 9000 Ghent, Belgium; E-mail: pascal.boecxk@ugent.be

[4] Systemic Physiological and Ecotoxicological Research (SPHERE), Antwerp University, Groenenborgerlaan 171, 2020 Antwerp, Belgium; E-mail: lieven.bervoets@uantwerpen.be

[5] Toxicological Centre, University of Antwerp, Universiteitsplein 1, 2610 Wilrijk, Belgium; E-mail: adrian.covaci@uantwerpen.be

**Corresponding author:**

Dr. Jens De Meyer

Evolutionary Morphology of Vertebrates - Ghent University

K.L. Ledeganckstraat 35

9000 Ghent (Belgium)

Telephone : +329 264 52 20

E-mail : Jendmeye.demeyer@ugent.be

**ABSTRACT**

Several aspects of the life cycle of the critically endangered European eel (*Anguilla anguilla*) remain poorly understood. One such aspect is the broad- versus narrow-head dimorphism, and how this impacts their overall performance at different stages of their life cycle. At the yellow eel stage, the phenotypes show a trophic divergence. We investigated whether pollutant accumulation is affected by this disparity. We show that broad-headed eels contained higher concentrations of mercury and several lipophilic organic pollutants, compared to narrow-headed ones, irrespective of their fat content. The hereby confirmed link between the phenotypic disparity, its associated feeding ecology and its impact on pollutant accumulation thus raises further concerns about their migratory and reproductive success. Considering that pollution is an important contributor to the European eel's decline, our results demonstrate that broad-headed eels are more vulnerable to detrimental pollutant accumulation. This compromises their successful contribution to their population's reproduction and its restoration.

**Keywords :** Pollution – Biomagnification – Dimorphism – POPs – Trace metals

**CAPSULE**

Pollutant uptake rate in European eel can be governed by trophic segregation associated with morphological specialization, with the rate depending on the contaminants lipophilicity.

**INTRODUCTION**

While European eels (*Anguilla anguilla*) have been studied extensively, many questions regarding their unique life cycle still remain unanswered. Dependent on oceanic current dynamics, this catadromous fish arrives as an un-pigmented glass eel at the continental waters of Europe (*1*). They continue their journey up the rivers, where they feed and grow into yellow

eels. For several years, they accumulate a fat reserve of at least 12% of their body weight, which is required for their migration back across the ocean and for gonadal development, to become the mature silver eels that will eventually spawn in the Sargasso Sea (*2, 3*). Worryingly, the analysis of the current glass eel recruitment indices at European monitoring stations have revealed a decrease to only 1%, compared to the late 1970's, in the North Sea region and to less than 5% in the rest of Europe (*4*). Consequently, the European eel is considered critically endangered on the International Union for Conservation of Nature (IUCN) red list. Following the EU Eel Regulation put in place in 2007 to restore the European eel stock (Council Regulation (EC) No. 1100/2007), EU Member States have developed Eel Management Plans (EMPs) with the objective to obtain a silver eel biomass escapement of 40%, compared to a situation without anthropogenic disturbances. Alarmingly, more than 50% of the current EMP progress reports show a failing to meet this target (*5*), indicating that much more effort is needed to be put wards the European eel's recovery. A thorough understanding of its ecology is thereby crucial to develop proper management measures. Among other factors, such as habitat loss (*6*), migration barriers (*7*), parasites (*8*), overfishing (*9*), climate change and changes in oceanic conditions (*10, 11*), the accumulation of pollutants could be one of the possible synergistic causes that are contributing to the decline of the eel population (*12*).

Eels bio-accumulate many lipophilic pollutants in their fat tissue throughout their life. When eels start migrating and turn into silver eels, they stop feeding and thrive on their fat reserves. The continuous fat burning, in combination with endocrine-induced morphological and physiological changes during migration, induces a remobilization of pollutants into the bloodstream and leads to a subsequent increase in tissue concentrations of target organs, such as the developing gonads (*13-15*). Bio-accumulation of toxic compounds can lead to physiological disturbances, lowered resistance, disturbed reproduction and possibly even

death, before eels reach the spawning area (*14, 16*). Even when eels successfully complete the migration, evidence has shown that 17-52% of the original fat reserves, together with its pollutants, are incorporated in the oocytes. This maternal transfer of contaminants to eggs is expected to increase the mortality of larvae, especially when the eels come from highly polluted environments (*17*). Thus, pollution impacting physiological processes during the European eel's life cycle is thought to be a crucial factor contributing to their decline.

While eels can absorb pollutants through their gills and skin, the major uptake of Persistent Organic Pollutants (POPs) and trace metals, such as mercury, occurs through the ingestion of contaminated food. European yellow eels demonstrate trophic divergence which is associated with a head shape dimorphism: broad-headed eels consume more fish and crustaceans, whereas narrow-headed eels mainly feed on benthic invertebrates (*18-21*). Also anatomically, the dimorphism involves variation in the musculoskeletal components of the feeding apparatus, which increases biting performance in broader heads (*22*). Here, we investigated whether this disparity in trophic ecology could also affect the accumulation of pollutants, which could alter reproductive ability. We hypothesize that broad-headed eels, which feed higher in the food chain (*23*), are more vulnerable to pollutant accumulation and are thus more susceptible to the detrimental pollutant effects, due to the consumption of more contaminated prey. Gaining insight into the interaction of the eel's morphology with its feeding ecology and pollutant accumulation would not only be a key element for improving recovery efforts, but it would also shed some much needed light onto how feeding-associated morphological variation can cause differential pollutant accumulation in eels.

## MATERIAL AND METHODS

### 1. Experimental design

#### *1.1 Sample collection*

European eels (N = 377) were captured by fyke nets and electric fishing in Lake Weerde (Belgium) in October 2015. Lake Weerde is a small (14 ha) lake in the Scheldt catchment, which is located in a recreational and agricultural area, with no important industrial activity. There is no open connection to a river system and all eels originated from glass eel restocking. It was initially a lake with a depth of approximately 8 m, resulting from sand excavation between 1968 and 1973. In order to create a more shallow lake with different shallow water zones to increase biodiversity, 250 000 $m^3$ of inert demolition material was used to partially fill the lake during the 1990s. However, apparently, also toxic material had been dumped, resulting in Lake Weerde being a highly contaminated lake for polychlorinated biphenyls (PCBs) and other contaminants (considering the Flanders Eel Pollution Monitoring Network). Because of these conditions, this lake was chosen for the present study. By annual monitoring, it was shown that PCB body burden of eels were decreasing from 1998 to 2005 (24). However, a steep increase of PCB contamination was observed in 2006, which was suspected to be due to a local discharge or spilling of toxic waste containing PCBs (25).

All eels were anaesthetized with MS222 (Tricaine methanesulfonate). Subsequently, total length (TotL) and total weight (W) were measured. Additionally, pictures of the head were taken in dorsal view and head width (HW) was measured between the jaw hinges at the nearest 0.1 mm, using a Mauser digital caliper. HW/TotL was calculated in the field. Eye size was used to determine whether an eel was in the yellow or silver eel stage, as eye size increases extensively during silvering (26). Out of the 377 eels, 75 yellow eels were selected over a wide range of HW/TotL for further analyses. All the selected eels were larger than 46

cm ($TotL_{min-max}$: 46.5 – 67 cm), and thus were also all female (27), hence a sex effect could be excluded. The other eels were released again into the wild once they had recovered from anesthesia. The condition of the 75 eels was determined by calculating the Le Cren's condition factor K (28) as follows: K = W/W' where W is the observed weight and W' the calculated weight based on the length-weight relationship ($W = a \times TotL^b$, where a is the intercept of the slope and b the slope of the relationship). Subsequently, the 75 eels were anaesthetized by MS222 and euthanized by an MS222 overdose, in accordance with the Belgian legislation. The eels were decapitated and the heads were fixed in 10% formalin and preserved in 70% ethanol. The body was skinned, intestines were removed and after decapitation, the body was cut into four equal parts. The muscle tissue of the first three parts was used for further analyses, while the final part acted as a reserve (figure S3). The muscle tissue of the first part was used for stable isotope analysis, while the muscle tissue of the second part was used for analysis of Persistent Organic Pollutants and the third part for the analysis of trace metals. This protocol has been applied according to the methods developed by INBO during the Eel Pollution Monitoring Network in Flanders (29) and described in ICES (30). It has been further used during other international eel assessments (31, 32).

***1.2 Head shape determination***

We used a mixture analysis in PAST to visualize a bimodal distribution, based on the HW/TL of the selected eels. We selected the point where the two unimodal distributions of the frequency histogram overlapped as the separation value between broad- and narrow-heads. The separation value was found at a HW/TL of 0.030. Based on this value, we considered eels with a HW/TL lower than 0.0275 as narrow-heads, eels with a HW/TL higher than 0.0325 as broad-heads and eels with a HW/TL between these values as intermediates. Using these cut-

144 off values, our dataset consisted of 26 narrow-heads (NH), 25 intermediates (INT) and 24
145 broad-heads (BH).

146 **2. Analyses**

147 ***2.1 Age determination***

148 The left and right sagittal otoliths were removed from the head, to determine the age of the
149 eels by the burning and cracking method (33, 34). This method is recommended for eel ageing,
150 especially for large eels (35). In short, the otoliths were first cut into two equal pieces and
151 were subsequently burned in a flame, revealing the annuli on the broken face. The otoliths
152 were then mounted cut face up onto a glass slide in silicone. Pictures of the otoliths were
153 taken using an SZX9 stereomicroscope, equipped with a ColorView 8 digital camera (Olympus,
154 Tokyo, Japan). These pictures were then used to determine the age of each eel. The age of
155 each eel was determined independently by two researchers in order to decrease possible
156 errors.

157 ***2.2 Body part 1: Stable isotope analyses***

158 One body part was used to obtain approximately 10 g of muscle tissue. These samples were
159 immediately frozen in liquid $N_2$ at -80°C and sent to ISOFYS (Isotope Bioscience lab, Ghent
160 University, Belgium), where they were stored in a freezer at -24°C. For analyses, the muscle
161 tissue was dried in an oven at 60°C for at least 48 h. The dried muscle tissues were then
162 completely homogenized and 100 µg per sample was used for stable isotope analyses. Total
163 N and $\delta^{15}N$ were measured using an elemental analyzer (ANCA-SL, SerCon, UK) coupled to an
164 isotope ratio mass spectrometer (20-22, SerCon, UK) (EA-IRMS). We used casein (%N = 13.32
165 and $\delta^{15}N$ = 5.94 per mil (Elemental Micro-analyses, UK)) as a laboratory standard that was
166 certified against NIST cysteine 143d for %N and IAEA-CH-6 for $\delta^{15}N$.

167 ***2.3 Body part 2: Persistent Organic Pollutants (POPs)***

The second body part of the eels was also stored in a freezer at -20°C and sent to the Toxicological Centre of Antwerp University. Lipids and POPs were extracted and quantified according to the method described by Malarvannan et al. (36). The measured analytes included 36 PCB congeners (IUPAC numbers 18, 28, 31, 44, 47, 49, 52, 66, 70, 74, 87, 95, 99, 101, 105, 110, 118, 128, 138, 146, 149, 151, 153, 156, 167, 170, 171, 177, 180, 183, 187, 194, 196, 199, 206, 209), 7 PBDE congeners (IUPAC numbers: 28, 47, 99, 100, 153, 154, 183), three DDTs (*p,p'*-DDT, *p,p'*-DDD and *p,p'*-DDE), hexachlorobenzene (HCB), three HCBDs (α-, β- and γ- isomers), cis- and trans-nonachlor (CN and TN, respectively), cis- and trans-chlordane (CC and TC), oxychlordane (OxC) and anti- and syn-Dechlorane Plus (a-DP and s-DP). In short, a homogenized sample of approximately 1 g eel muscle (ww) was weighed, then mixed with anhydrous $Na_2SO_4$ and spiked with internal standards (BDE 77, BDE 128, $^{13}$C-BDE 209, CB 143 and $^{13}$C-HBCDs). Next, the samples were extracted for 2h by hot Soxhlet with 100 ml hexane/acetone (3:1; v/v) and cleaned up on acidified silica. The lipid content was determined gravimetrically on an aliquot of the extract (105 °C, 1 h). The remaining extract was cleaned on 8 g of acidified silica (44%) and the analytes were then eluted with 20 mL hexane and 15 mL dichloromethane. The cleaned extract was concentrated to near dryness under a gentle nitrogen stream, re-dissolved in 0.5 mL hexane and loaded on silica cartridges (500 mg/3 mL, Agilent). The first fraction was eluted with 6 mL hexane and contained PCBs, DDTs, CHLs, HCB, PBDEs and DPs, whereas the second fraction, containing the HBCDs, was eluted with 8 mL DCM. Both fractions were evaporated to near dryness. The first fraction was re-solubilized in 100 µL iso-octane, while the second was re-solubilized in 100 µL methanol. PCBs, DDTs, CHLs, HCB, PBDEs and DPs were analysed by GC-MS, whereas the HBCDs were quantified by LC-MS/MS (25, 37). The detection limit was 0.05 ng/g ww for the PBDEs, 0.2 ng/g ww for the

lower chlorinated PCBs (CB18-CB66), 0.3 ng/g ww for the DDTs, and 0.1 ng/g for the remaining analytes.

The POP analysis was evaluated by measuring the absolute recoveries of the internal standards. Two criteria were used to quantify the peaks as target compounds. First, the retention time of the peak had to match the retention time of the standard compound within ± 0.1 min. Secondly, a signal-to-noise ratio (S/N) of 3:1 or higher was required. We determined the *limit of quantification (LOQ)* by multiplying the standard deviation of the mean of the blank measurements by three. Each batch contained seven samples and a procedural blank. The latter was needed in order to detect possible interferences and/or contamination by solvents, reagents or glassware. As consistent procedural blanks, with an RSD below 30%, were obtained, we calculated the mean blank value of each compound. The values in the samples were then subtracted by this mean value. The internal standard PCB 143 had a mean ± SD recovery of 86 ± 6%, while the recovery was 93 ± 10% for BDE77. In order to validate the analytical procedures, we analyzed the certified material SRM 1945 (organic contaminants in whale blubber) which deviated less than 10% from certified values.

### *2.4 Body part 3: Trace metals*

The third body part of the eels was stored in a freezer at -20 °C and sent to SPHERE (Systematic Physiological & Ecotoxicological Research, University of Antwerp, Belgium). Of this body part, 0.5 g wet weight (ww) of homogenized fish muscle tissue was accurately weighed. Digestion and analysis of the samples was done according to Mataba et al. (38). Dry weight (dw) was determined after freeze drying. 1500 µL of HCl (37%), 500 µL of concentrated $HNO_3$ (69%), 200 µl $H_2O_2$ and a magnetic stirrer were added to each of the samples. The samples were subsequently digested using a SP-Discover microwave (CEM, USA) in two steps. The first step ran at 120 °C, ramp and hold time of five minutes, with a maximum pressure of 34 bars at

300W and low stirring. Step 2 was identical to step 1 but ran at 160°C. To analyze Hg, the samples were diluted upon 5-6% acid, whereas 1-2% acid was used for the other trace metals (zinc, lead, nickel, copper, chromium, cobalt, cadmium and arsenic).

In order to control the quality, blanks and certified reference material (CRM) were added and processed identical to the other samples. As CRM, both lyophilised Cod Muscle (BCR 422) provided by the Institute for Reference Materials and Measurements (IRMM, Geel, Belgium) and freeze dried muscle tissue (no. 2976) from NIST (National Institute of Standards and Technology-USA) were used.

Subsequently, all eel samples were analyzed for total mercury in cold plasma mode by High Resolution Inductively Coupled Mass Spectrometry (HR-ICP-MS; Thermo scientific Finnigan element 3, Waltham, MA, USA), which has an instrumental detection limit of 0.01 µg/L. An Inductively Coupled Plasma-Mass Spectrometer (ICP-MS, Varian UltraMass 700, Victoria, Australia), with a detection limit of 0.1 µg/L, was used to measure the concentrations of the remaining trace metals. The obtained concentrations are very similar to the certified concentrations in the reference material, with a range from 90 to 110%, depending on the metal.

## 3. Data analysis

Analytes that were below detection limit (BDL) in more than 50% of the specimens were not used for further analysis (Table S1). Consequently, the BDEs 28, 99, 153, 154 and 180, the β- and γ- isomers of HBCD and the trace metals Cd, Co and Ni were not used. Measurements that were BDL in the remaining pollutants were estimated as detection limit*1/2. We need to note, however, that the replacement of censored values by an arbitrary one, may have an influence on the given means and standard deviation (Helsel, 2012). While little influence is

239 expected for the pollutants α-hexabromocyclododecane (α-HBCD; only 4% of the eels BDL),
240 HCB (4%) and BDE100 (1%), the replacement of the censored values could be more
241 pronounced for OxC (27%), Cr (23%), *p,p'*-DDT (20%) and TN (11%). Six PCBs (IUPAC numbers
242 28, 52, 101, 138, 153 and 180) and their sum were used for further statistical analysis, as these
243 are used to control for food safety according to European legislation. In addition, the sum of
244 *p,p'*-DDD, *p,p'*-DDT and *p,p'*-DDE (∑DDT) was determined as a proxy of total DDTs.
245 A Shapiro-Wilk test was performed to investigate whether age, total length, weight, trophic
246 position, condition and fat content followed a normal distribution in the different phenotypes
247 (BHs, INTs and NHs). In case the assumptions were met, an ANOVA was performed to test
248 whether these variables differed significantly between the three phenotypes. If the data were
249 not normally distributed, a non-parametric permutation test (10,000 replicates) was used. In
250 addition, the measurements of these variables were log-transformed and were then used for
251 a Between-group Principal Component analysis (PCA) to find potential differences between
252 the phenotypes
253 Next, the lipid weight concentrations of the different POPs and the wet weight concentrations
254 of the trace metals were log-transformed. Subsequently, a Shapiro-Wilk test was performed
255 to test whether these concentrations in each phenotype followed a normal distribution.
256 Potential outliers were identified by performing a mixture analysis. In case one specimen
257 differed strongly from all the others, it was removed for further analysis. In case multiple
258 outliers were present, we performed non-parametric tests. Subsequently, we calculated the
259 Pearson (if data were normally distributed) or Spearman's ranked (if data were not normally
260 distributed) correlation between POPs (lipid weight basis), metals (wet weight basis), age and
261 TotL.

Furthermore, in case a normal distribution was not supported, we used a non-parametric permutation test (10,000 replicates) to detect significant differences in the log-transformed pollutant concentrations between the different phenotypes. When the assumptions were met, an ANCOVA was performed to find significant differences in the log-transformed pollutant concentrations between the different phenotypes. The ANCOVAs were performed both with the log-transformed total length (TotL) and age as co-variate.

In addition, a between-group PCA were performed on the log-transformed lipid weight concentrations of the POPs.

Finally, we determined the mean lipid weight POPs concentrations in the three phenotypes and then calculated the mean(INT)/mean(NH) and mean(BH)/mean(INT) ratios. These were then plotted against the log(Kow)-values of these POPs (39-42). This allowed for a simplified data model, and comprehensible graphical representations, in order to clearly visualize POP behaviour over the different phenotype groups. Kow represents the octanol/water partition coefficient and the higher this value, the more hydrophobic (and thus lipophilic) a chemical is. For the POPs that included eels with concentrations BDL (OxC, TN, HCB, α-HBCD, *p,p'*-DDT and BDE100), we performed a sensitivity analysis by replacing the censored value by the minimum-value (0), by detection limit*1/2 and by the detection limit and then calculating the means of each phenotype. In case different patterns were observed, depending on the replacement value, the POP was not used for this analysis.

## RESULTS

### Head shape and trophic position

Based on the head width/total length ratio (HW/TotL), 26 narrow-headed (NH), 25 intermediate (INT) and 24 broad-headed (BH) female yellow (size class: 46.5 – 67cm) eels were selected. These groups did not differ significantly in total length, condition factor and body

286 weight. Intermediates were, however, significantly younger (Table 1). The fat content of NHs
287 was significantly higher compared to INTs and BHs (Table 1). Accordingly, a significant,
288 negative correlation was found between HW/TotL and fat content (r=-0.36; $P < 0.01$; Figure
289 1A). Trophic position (measured as $\delta^{15}N$), on the contrary, was positively correlated with
290 HW/TotL (r=0.66; $P < 0.01$; Figure 1B), but showed no correlation with TotL (r=-0.07; $P = 0.57$).
291 The $\delta^{15}N$ concentrations were significantly higher in BHs compared to INTs, while the
292 concentrations of the latter were significantly higher compared to NHs (Table 1). The
293 difference in average $\delta^{15}N$ between BHs and NHs equalled only 2.82‰, indicating that the
294 different phenotypes were less than one trophic position apart (43), which corresponds to
295 results obtained previously (*23*). Rather, the increase of $\delta^{15}N$ with HW/TotL indicates that eels
296 with a broader head consume relatively more prey items that are higher in trophic position.
297 This observation is supported by the literature, where a shift in $\delta^{15}N$ from 3.0 to 3.6 in omul
298 (*Coregonus migratorius*), for example, suggested that this fish did not only feed on benthic
299 invertebrates, but also on carnivores and omnivores (44). Our observations are also consistent
300 with the results obtained from stomach analyses, which indicated that broad-headed eels
301 consume proportionally more, but not exclusively larger prey items, such as fish and
302 crustaceans (*2*). The above described results are consistent with those of the between-group
303 PCA (Figure S1)

304 **Head shape and pollution**

305 Because of the lipophilic nature of POPs (45), we used the lipid-normalized concentrations
306 (expressed as ng/g fat) for our analyses. This also prevented a confounding effect of
307 differences in fat content. Several pollutants were found to be below the detection limit in
308 more than 50% of the eels and were, therefore, not included for further statistical analyses
309 (Table S1). Furthermore, of all measured PCBs, only the six ICES indicator PCBs and their sum

were included for further analyses (CB 28, 52, 101, 138, 153 and 180). The median ± SD of the pollutant concentrations is found in Table S2. None of the pollutants correlated with size or age (Table S3). The results of the ANCOVA with TotL and age were comparable (Table 2). For *p,p'*-DDE and –DDT, BDE47 and 100, OxC and TN, a non-parametric permutation test was used since these data did not fall within a normal distribution (Table S4). HCB concentrations were found to be significantly lower in eels with a broader head. The concentrations of the higher chlorinated PCBs (CB 138-180), *p,p'*-DDE, *p,p'*-DDT and both ∑PCB and ∑DDT were found to be similar between INTs and BHs, with only the concentrations of the higher chlorinated PCBs and *p,p'*-DDT being highest in BHs, although for the latter, the median is used (Table 2-3). These concentrations were significantly higher compared to NHs. The *p,p'*-DDD, BDE100 and CB101 concentrations, on the other hand, were comparable between NHs and BHs, with higher values measured in INTs. Finally, BDE47 and α-HBCD, OxC and TN differed strongly between the three groups, with the concentrations being significantly higher in INTs (Table 2-3). Interestingly, the mean concentration of α-HBCD and BDE47 and the median concentration of OxC and TN were generally the highest in INTs.

However, the between-group PCA on the log-transformed pollutant concentrations indicated that PC1 scores showed a lot of variation in BHs (Figure 2). The lower mean values of BHs, compared to those of INTs, resulted from some BHs having low pollutant concentrations. Furthermore, the between-group PCA indicated that BHs were generally characterized by a combination of lower PC1-scores and higher PC2-scores, while the opposite was true for NHs. INTs take up a rather intermediate morphospace. As such, BHs are mainly associated with higher concentrations of higher chlorinated CBs (CB 138, 153, 180), *p,p'*-DDE and *p,p'*-DDT, whereas NHs have a higher amount of CB28, α-HBCD and especially HCB. While INTs also have

high pollutant concentrations, these concentrations are not as high as in BHs or NHs (as PCA shows).

Interestingly, the compounds with the highest concentrations in BHs are also the most lipophilic ones. Therefore, the mean POP concentrations (not log-transformed) of NHs, INTs and BHs were determined and used to calculate the mean(INT)/mean(NH), mean(BH)/mean(INT) and mean(BH)/mean(NH) ratios. The sensitivity analysis showed only different patterns for TN depending on the value by which a concentration BDL was replaced and was therefore not included in this analysis (Table S5). All three ratios were significantly positively correlated with lipophilicity (Kow; r=0.84, r=0.83 and r=0.88 for INT/NH, BH/INT and BH/H respectively; $P < 0.01$ in all cases*;* figures 3 and S2), indicating that the more lipophilic a pollutant is, the higher its concentration will be in broad-headed eels. Lipophilicity has also been related to bio-magnification potential, i.e. the more lipophilic a chemical is, the more likely it is to accumulate in food chains (45, 46). As such, the positive correlation between the POP ratios and lipophilicity can be explained by differences in prey consumption, since the studied eels did not differ in age, length or sex, except for the significantly younger age of INTs compared to BHs and NHs. This indicates that the proportionally higher consumption of such prey items leads to a cumulative uptake of highly lipophilic pollutants, which is consistent with previous studies suggesting that the uptake of such pollutants occurs through food (47, 48).

Finally, to analyze the accumulation of trace metals, wet weight muscle concentrations (ng/g eel) were used. Of all trace metals, only the measurements of mercury (Hg) and zinc (Zn) followed a normal distribution (Table S4). According to the ANCOVA with Totl and age as co-variate, the mercury concentrations were found to be significantly higher in BHs, compared to INTs and NHs (Table 2), whereas no significant differences were found for Zn. Using a permutation test, we also found that copper (Cu) concentrations were significantly higher in

BHs, compared to NHs (Table 3). Chromium(Cr) and arsenic (As), on the other hand, were found to be significantly lower in BHs, compared to NHs. Arsenic mainly accumulates in the exoskeleton of small invertebrates (49). Consequently, the higher consumption of these invertebrates by NHs could explain this observation. Lead (Pb) concentrations were found to be significantly lower in NHs compared to INTs, but did not differ significantly from BHs. The results of the trace metal analysis were thus consistent with results obtained previously, showing that Hg demonstrates a tendency to bio-magnify in food chains (50), whereas this is generally not the case for the other metals (51). Moreover, most metals are hydrophilic and will be taken up via the water rather than via the food. Additionally, most metals accumulate in the organs rather than in the muscle tissue (38). Together with Hg, the only exception in our study is Cu, which also increased with head width and thus trophic position.

Our novel findings show that there is a link between head shape, trophic position and pollutant accumulation. Eels with broader heads feed more on prey items which are higher up in the food chain, leading to an increased uptake of more lipophilic POPs and Hg, compared to eels with a narrower head.

## DISCUSSION

A driver for phenotypic-trophic disparity in European yellow eels could be to alleviate the pressure on food competition, thus increasing their survival rates (52). Additionally, a recent study has indicated that eels can adapt to differences in diet; young eels that were given hard prey, such as crustaceans, developed broader heads than eels that were given soft prey, such as chironomid larvae (53). The broader heads were associated with larger jaw muscles that facilitate consumption of hard prey (*22*). The capability to show such an adaptive, phenotypic response to differences in food accessibility and the decrease in intra-specific competition through this dimorphism are likely to increase the eel's survival. As such, the dimorphism

could be sustained in the population through natural selection, and thus be considered as adaptive. However, our results suggest that the causality between diet and head shape also controls the pollutant accumulation. Anthropogenic influences may thus turn an adaptive trait into a maladaptive one, as the advantage of adapting towards consuming larger and harder preys in the broad-headed yellow eel may ultimately lead to a lower reproduction potential as silver eel, due to increased pollutant accumulation (*17*).

While measurements of fat content in a particular subsample of muscle tissue may not be representative for the complete fish (54), we observed that the fat content of broad-head eels was significantly lower than that of NHs. This phenomenon could be explained by the trophic difference, with broad-head eels feeding proportionally more on larger and harder prey items, such as fish and crustaceans. The consumption of such larger prey is energetically more profitable than the consumption of small, benthic invertebrates (55). However, obtaining such prey items requires biting or spinning behaviour, in contrast to NHs sucking in small, benthic invertebrates. It has been demonstrated that the net energy gain when using biting and spinning behaviour is lower than when relying on suction feeding (56). It is thus possible that the observed differences in fat content are a consequence of the different feeding methods. Secondly, it is possible that prey items, such as benthic invertebrates, are more abundant and thus easier to capture than the more evasive fish and crustaceans and that NHs hence require less energy for prey capture.

Alternatively, several pollutants could have a negative impact on the eel's fat content, for example due to a higher energy demand induced by chemical stress (*14, 16*). The lower lipid energy reserves of BHs may thus also be a consequence of significantly higher concentrations of the more lipophilic pollutants (57). The measured lower fat content of BHs could, in turn, imply that BHs will also require a longer time to accumulate enough fat to start migration due

405 to pollution. Indeed, while similar in age, 54% of the NHs had accumulated enough fat (12%
406 of body weight (*3*)) to start migrating, while this was only 17% for the BHs. For INTs, this was
407 28%, but they were significantly younger. Pollution therefore may affect the BHs at four levels.
408 Firstly, during the fat accumulation period as yellow eels, where BHs need considerably more
409 time to accumulate enough lipid energy to migrate successfully. A delayed migration
410 inevitably increases the risk of being killed by predators or other factors. Secondly, if BHs
411 would still start their migration as silver eels, but with low fat concentrations, energy storage
412 would potentially be insufficient to fuel the transatlantic migration and production of
413 gametes, and thus leads to lowered reproduction potential (57). Thirdly, BHs have a higher
414 risk of being exposed to the detrimental effects of higher concentrations of pollutants, when
415 fat is being metabolised during migration. These effects may include disturbances of the
416 immune, reproductive, nervous and endocrine systems (*14*). Finally, being more loaded with
417 the most toxic pollutants, such as PCBs, could have a negative impact on the mean weight of
418 eggs by interfering with the development of the ovaries (58), possibly resulting in less viable
419 eggs. Our results therefore strongly indicate that BHs are expected to suffer more from POP
420 and mercury pollution than NHs at several (potentially cumulative) concentrations, due to the
421 trophic ecology related to head shape disparity. Additionally, the eel's head morphology has
422 also been related to parasite infection, showing that the higher piscivorous behavior of BHs
423 leads to a higher exposure and thus infection with the parasite *Anguillicoloides crassus* (59).
424 This parasite damages the swim bladder and drains the eel's energy by sucking blood, thus
425 also impairing the eel's migration success (8, 60). So, while natural selection would favour
426 dimorphism because of decreased intra-specific competition, anthropogenic effects may well
427 disrupt this adaptive process in polluted areas as the reproduction potential of BHs is expected
428 to be lower than that of narrow-heads. This is especially worrisome since current eel

restoration measures in the EU member states focus on producing maximal quantities of silver eels leaving the river catchments (at least a 40% silver eel biomass escapement), and do not take into consideration their overall body quality. It has been argued, however, that also the health status of silver eels should be improved at the level of pollution load, infection levels by pathological agents and fitness indicators, such as lipid levels and condition. These are all factors that are crucial for maximizing the eel's reproductive potential, and hence for the successful restoration of the European eel stock. Our results indicate that there could be differences in reproductive potential between broad- and narrow-headed eels from polluted environments. We would advise that the current stock assessment, which is based on quantitative indicators, should be jointly merged with indicators characterizing the quality of the eels leaving our catchments. This could potentially lead to an overall, much needed, successful restoration of European eel stocks.

**Acknowledgements**

We thank the personnel of INBO (Instititute for Nature and Forest Research) for their help with collecting and processing the eels. We thank K. Van Nieuland for her help with preparing the stable isotope analysis. This research was supported by BOF (Special Research Fund; BOF 01J05213 and BOF 13/24J/052).

**References**

1. Baltazar-Soares M*, et al.* (2014) Recruitment Collapse and Population Structure of the European Eel Shaped by Local Ocean Current Dynamics. *Curr. Biol.* 24:104-108.
2. Tesch FW (2003) *The eel* (Oxford: Blackwell Science) 5th Ed.
3. Van den Thillart GEEJM, Palstra AP, & van Ginneken VJT (2007) Stimulated migration of European silver eel: swim capacity and cost of transport. *J. Mar. Sci. Technol.* 15 (special issue):1-16.
4. ICES (2016) ICES WG Eel report - Report of the Working Group on Eels (WGEEL). (Cordoba, Spain).
5. ICES (2013) Report of the Workshop on Evaluation Progress Eel Management Plans (WKEPEMP). (ICES, Copenhagen, Denmark), p 759.

6. Kettle AJ, Asbjørn Vøllestad L, & Wibig J (2011) Where once the eel and the elephant were together: decline of the European eel because of changing hydrology in southwest Europe and northwest Africa? *Fish Fish.* 12:380-411.
7. Durif C, Elie P, Gosset C, Rives J, & Travade F (2002) Behavioral study of downstream migrating eels by radio-telemetry at a small hydroelectric power plant. *Am. Fish. S. S.* 33:343-356.
8. Palstra AP, Heppener DFM, van Ginneken VJT, Székely C, & van den Thillart GEEJM (2007) Swimming performance of silver eels is severely impaired by the swim-bladder parasite Anguillicola crassus. *J. Exp. Mar. Biol. Ecol.* 352:244-256.
9. Dekker W (2003) On the distribution of the European eel (Anguilla anguilla) and its fisheries. *Can. J. Fish. Aquat. Sci.* 60:787-799.
10. Friedland KD, Miller MJ, & Knights B (2007) Oceanic changes in the Sargasso Sea and declines in recruitment of the European eel. *ICES J. Mar. Sci.* 64:519-530.
11. Bonhommeau S*, et al.* (2008) Impact of climate on eel populations of the Northern Hemisphere. *Mar. Ecol. Prog. Ser.* 373:71-80.
12. Belpaire C, Pujolar JM, Geeraerts C, & Maes GE (2016) Contaminants in Eels and their Role in the Collapse of the Eel Stocks. *Biology and ecology of anguillid eels*, ed Arai T (CRC Press - Taylor & Francis Group, Boca Raton, FL), pp 225-250.
13. Lewander K, Dave G, Johansson ML, Larsson A, & Lidman U (1974) Metabolic and haematological studies on the yellow and silver phases of the European eel, *Anguilla anguilla* L. – I. carbohydrate, lipid, protein and inorganic ion metabolism. *Comp. Biochem. Physiol.* 47B:571-581.
14. Geeraerts C & Belpaire C (2010) The effects of contaminants in European eel: a review. *Ecotoxicology* 19:239-266.
15. Freese M*, et al.* (2017) Maternal transfer of dioxin-like compounds in artifically matured European eels. *Environ. Poll.* 227:348-356.
16. Robinet T & Feunteun E (2002) Sublethal effects of exposure to chemical compounds: A cause for the decline in Atlantic eels? *Ecotoxicology* 11:265-277.
17. Foekema EM, Kotterman M, de Vries P, & Murk AJ (2016) Maternally transferred dioxin-like compounds can affect the reproductive success of European eel. *Environ. Toxicol. Chem.* 35:241-246.
18. Törlitz H (1922) Anatomische und entwicklungsgeschichtliche Beiträge zur Artfrage unseres Flussaales. *Z. Fisch* 21:1-48.
19. Thurow F (1958) Untersuchungen uber die spitz und breitköpfigen Varianten des Flussaales. *Arch. Fischereiwiss.* 9:79-97.
20. Lammens EHRR & Visser JT (1989) Variability of mouth width in European eel, Anguilla anguilla, in relation to varying feeding conditions in three Dutch lakes. *Environ. Biol. Fish.* 26:63-75.
21. Proman JM & Reynolds JD (2000) Differences in head shape of the european eel. *Fisheries Manag. Ecol.* 7:349-354.
22. De Schepper N (2007) Evolutionary Morphology of body elongation in teleosts: aspects of convergent evolution. PhD dissertation (Ghent University, Ghent, Belgium).
23. Cucherousset J*, et al.* (2011) Fitness consequences of individual specialisation in resource use and trophic morphology in European eels. *Oecologia* 167(1):75-84.
24. Belpaire C (2008) Pollution in eel: A cause of their decline? PhD thesis (Catholic University Leuven, Brussels).
25. Belpaire C, Geeraerts C, Roosens L, Neels H, & Covaci A (2011) What can we learn from monitoring PCBs in the European eel? A Belgian experience. *Environ. Int.* 37:354-364.
26. Pankhurst NW (1982) Changes in body musculature with sexual maturation in the European eel *Anguilla anguilla* L. . *J. Fish Biol.* 21:417-428.
27. Durif CMF, van Ginneken V, Dufour S, Müller T, & Elie P (2009) Seasonal evolution and individual differences in silvering eels from different locations. *Spawning migration of the European eel: Reproduction index, a useful tool for conservation management*, eds Van den Thillart G, Dufour S, & Rankin JC (Springer Netherlands), pp 13-38.

28. Le Cren ED (1951) The length-weight relationship and seasonal cycle in gonad weight and condition in the perce *Perca fluviatilis*. *J. Anim. Ecol.* 20:201-219.
29. Maes J, Belpaire C, & Goemans G (2008) Spatial variations and temporal trends between 1994 and 2005 in polychlorinated biphenyls, organochlorine pesticides and heavy metals in European eel (Anguilla anguilla L.) in Flanders, Belgium. *Environ. Pollut.* 153:223-237.
30. ICES (2015) Report of the Workshop of a Planning Group on the Monitoring of Eel Quality under the subject "Development of standardized and harmonized protocols for the estimation of eel quality" (WKPGMEQ). (ICES, Brussels, Belgium), p 274.
31. CORDIS (2013) Final Report Summary - EELIAD (European Eels in the Atlantic: Assessment of Their Decline ). (The Secretary of State for Environment, Food and Rural Affairs, Lowestoft, U.K.).
32. Pujolar JM*, et al.* (2012) Surviving in a toxic world: Transcriptomics and gene expression profiling in response to environmental pollution in the critically endangered European eel. *BMC Genomics* 13:507.
33. Hu LC & Todd PR (1981) An improved technique for preparing eel otoliths for aging. *New Zeal. J. Mar. Fresh.* 15:445-446.
34. Moriarty C (1973) A technique for examining eel otoliths. *J. Fish Biol.* 5:183-184.
35. ICES (2011) Report of the Workshop on Age Reading of European and American Eel (WKAREA 2). (ICES, Bordeaux, France).
36. Malarvannan G*, et al.* (2014) Assessment of persistent brominated and chlorinated organic contaminants in the European eel (Anguilla anguilla) in Flanders, Belgium: Levels, profiles and health risk. *Sci. Total Environ.* 482-483:222-233.
37. Roosens L*, et al.* (2010) Spatial variations in the levels and isomeric patterns of PBDEs and HBCDs in the European eel in Flanders. *Environ. Int.* 36:415-423.
38. Mataba GR, Verhaert V, Blust R, & Bervoets L (2016) Distribution of trace elements in the aquatic ecosystem of the Thigithe river and the fish *Labeo victorianus* in Tanzania and possible risks for human consumption. *Sci. Total Environ.* 547:48-59.
39. Hayward S, Lei Y, & Wania F (2006) Comparative evaluation of three high-performance liquid chromatography-based Kow estimation methods for highly hydrophobic organic compounds : polybrominated diphenyl ethers and hexabromocyclododecane. *Environ. Toxicol. Chem.* 25:2018-2027.
40. Kuramochi H, Maeda K, & Kawamoto K (2004) Physiochemical properties of selected polybrominated diphenylethers and comparison with some brominated aromatics and PCDDs. *Organohalogen Compounds* 66:2420-2425.
41. ATSDR (2004) Toxicological Profile for polybrominated biphenyls and polybrominated diphenyl ethers. (ATSDR (Agency for Toxic Substances and Disease Registry), Public Health Service, U.S. Department of Health and Human Services, Atlanta, GA).
42. Zhou W, Zhai Z, Wang Z, & Wang L (2005) Estimation of n-octanol/water partition coefficients (Kow) of all PCB congeners by density functional theory. *J. Mol. Struct.: THEOCHEM* 755:137-145.
43. Post DM (2002) Using stable isotopes to estimate trophic position: Models, Methods, and assumptions. *Ecology* 83:703-718.
44. Ohkouchi N, Ogawa NO, Chikaraishi Y, Tanaka H, & Wada E (2015) Biochemical and physiological bases for the use of carbon and nitrogen isotopes in environmental and ecological studies. *Prog. Earth Plan. Sci.* 2(1).
45. Kelly BC, Ikonomou MG, Blair JD, Morin AE, & Gobas FAPC (2007) Food Web-Specific Biomagnification of Persistent Organic Pollutants. *Science* 317(5835):236-239.
46. Borga K, Gabrielsen GW, & Skaare JU (2001) Biomagnification of organochlorines along a Barents Sea food chain. *Environ. Pollut.* 113:187-198.
47. Bremle G, Okla L, & Larsson P (1995) Uptake of PCBs in Fish in a Contaminated River System: Bioconcentration Factors Measured in the Field. *Environ. Sci. Technol.* 29:2010-2015.

48. Tapie N*, et al.* (2011) PBDE and PCB contamination of eels from the Gironde estuary: From glass eels to silver eels. *Chemosphere* 83(2):175-185.
49. Mason RP, Laporte J, & Andres S (2000) Factors controlling the bioaccumulation of mercury, methylmercury, arsenic, selenium, and cadmium by freshwater invertebrates and fish. *Arch. Environ. Con. Toxicol.* 38:283-297.
50. Atwell L, Hobson KA, & Welch HE (1998) Biomagnification and bioaccumulation of mercury in an arctic marine food web Insights from stable nitrogen isotope analysis. *Can. J. Fish. Aquat. Sci.* 55:1114-1121.
51. Cardwell RD, DeForest DK, Brix KV, & Adams WJ (2013) Do Cd, Cu, Ni, Pb, and Zn Biomagnify in Aquatic Ecosystems? *Rev. Environ. Contam. T.* 226:101-122.
52. Schoener TW (1974) Resource partitioning in ecological communities. *Science* 185:27-39.
53. De Meyer J, Christiaens J, & Adriaens D (2016) Diet-induced phenotypic plasticity in European eel (*Anguilla anguilla*). *J. Exp. Biol.* 219:354-363.
54. Persson ME, Larsson P, Holmqvist N, & Stenroth P (2007) Large variation in lipid content, ΣPCB and δ13C within individual Atlantic salmon (*Salmo salar*). *Environ. Pollut.* 145:131-137.
55. Galarowicz TL, Adams JA, & Wahl DH (2006) The influence of prey availability on ontogenetic diet shifts of a juvenile piscivore. *Can. J. Fish. Aquat. Sci.* 63:1722-1733.
56. Helfman GS & Winkelman DL (1991) Energy trade-offs and foraging mode choice in american eels. *Ecology* 72(1):310-318.
57. Belpaire C*, et al.* (2009) Decreasing eel stocks: survival of the fattest? *Ecol. Freshw. Fish* 18:197-214.
58. Johnson LL*, et al.* (1998) Contaminant effects on ovarian development and spawning success in rock sole from Puget Sound, Washingtion. *T. Am. Fish. Soc.* 127:375-392.
59. Pegg J, Andreou D, Williams CF, & Britton JR (2015) Head morphology and piscivory of European eels,Anguilla anguilla, predict their probability of infection by the invasive parasitic nematodeAnguillicoloides crassus. *Freshwater Biol.* 60:1977-1987.
60. Neto AF, Costa JL, Costa MJ, & Domingos I (2010) Epidemiology and pathology of Anguillicoloides crassus in European eel Anguilla anguilla from the Tagus estuary (Portugal). *Dis. Aquat. Organ.* 88:225-233.

## FIGURE CAPTIONS

**Figure 1 (1 column width): Relation between fat content and trophic position with relative eel head width.** A: Relation of fat content with eel head width relative to total length (HW/TotL). B: Relation of trophic position ($\delta^{15}N$) with eel head width relative to total length (HW/TotL). Light blue dots represents narrow-heads, blue dots intermediates and dark blue dots broad-headed eels. A representative of each phenotype is given above. Black dots represent the means of each phenotype; the error bars represent standard deviation.

**Figure 2 (1 or 1.5 column width): Between-group PCA on the log-transformed pollutant concentrations and the corresponding biplot**. The pollutant concentrations were expressed as lipid weight. Light blue dots represents narrow-heads, blue dots intermediates and dark blue dots broad-headed eels. The amount of variation explained by each Principal Component (PC) is shown in parentheses.

**Figure 3 (1 column width): Relation of the mean(BH)/mean(NH) ratio of the different pollutants plotted against the log of their octanol/water partition coefficient (Kow).** The pollutants are expressed as lipid weight. NH: Narrow-heads, BH: Broad-heads. Blue diamonds represent pentachlorobiphenyls (PCBs), green diamonds Dichlorodiphenyltrichloroethanes (DDTs) and red the remaining measured pollutants.

618 **FIGURES**

619 **Figure 1**

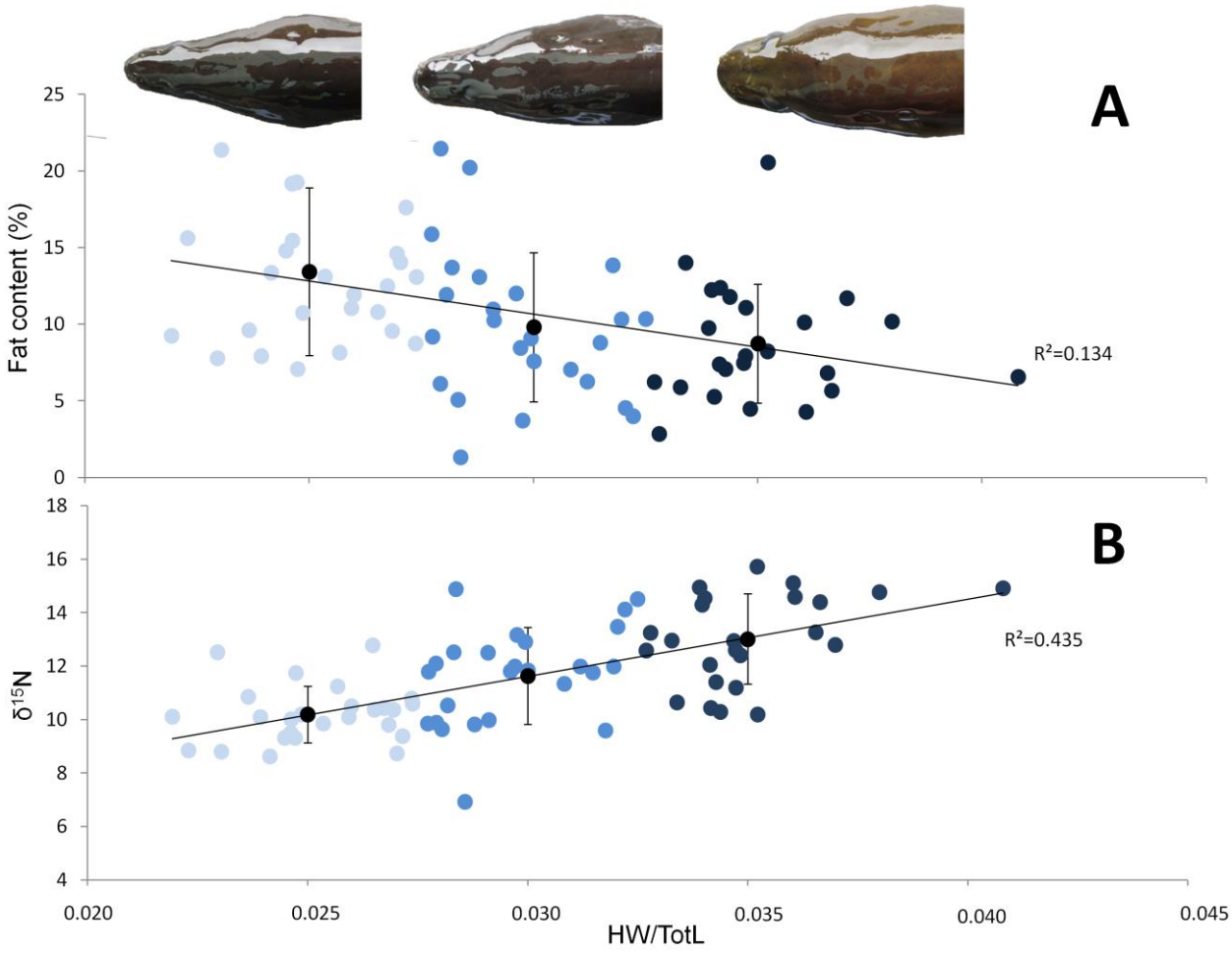


620

621

622 **Figure 2**

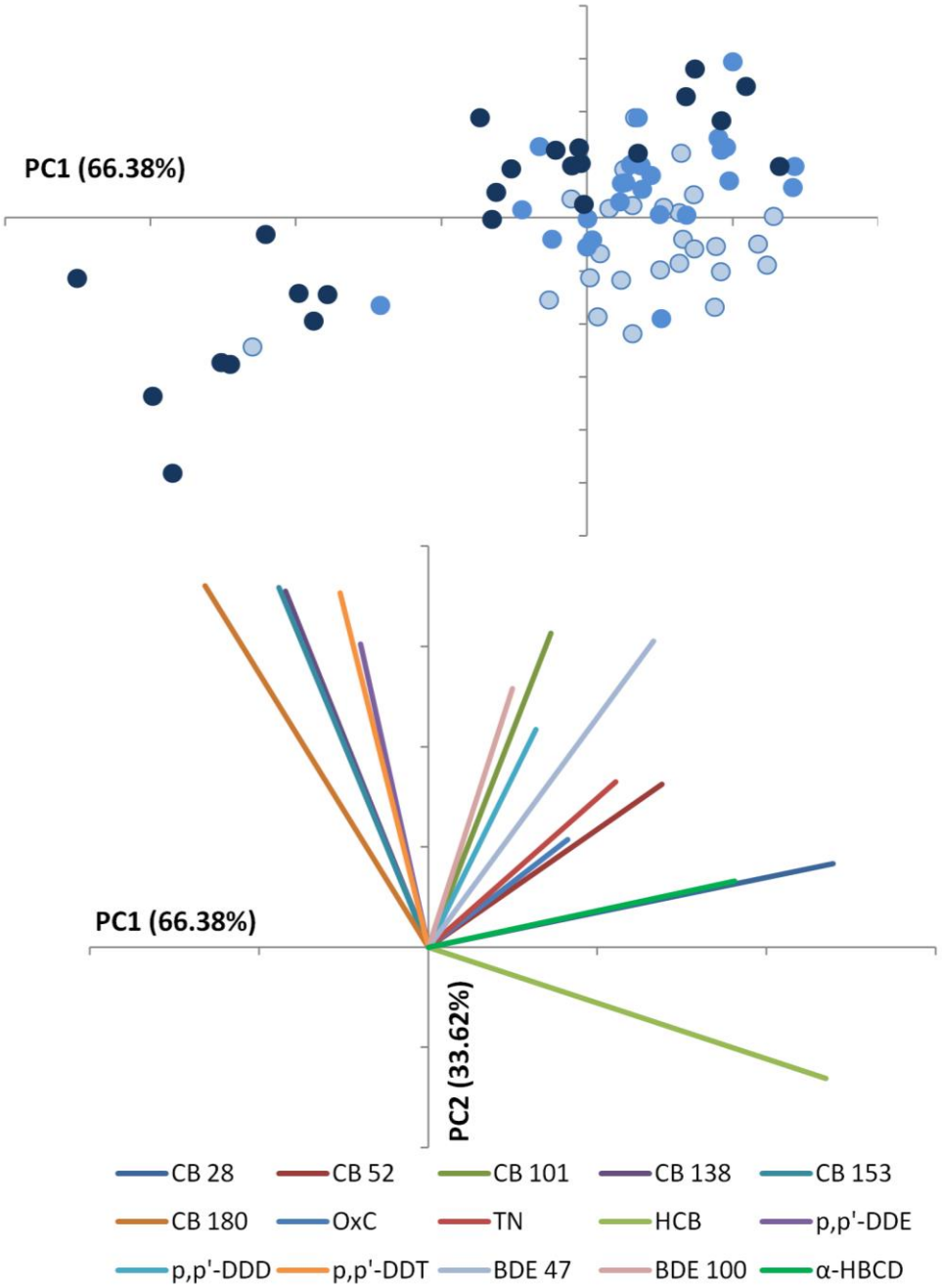


623

624 **Figure 3**

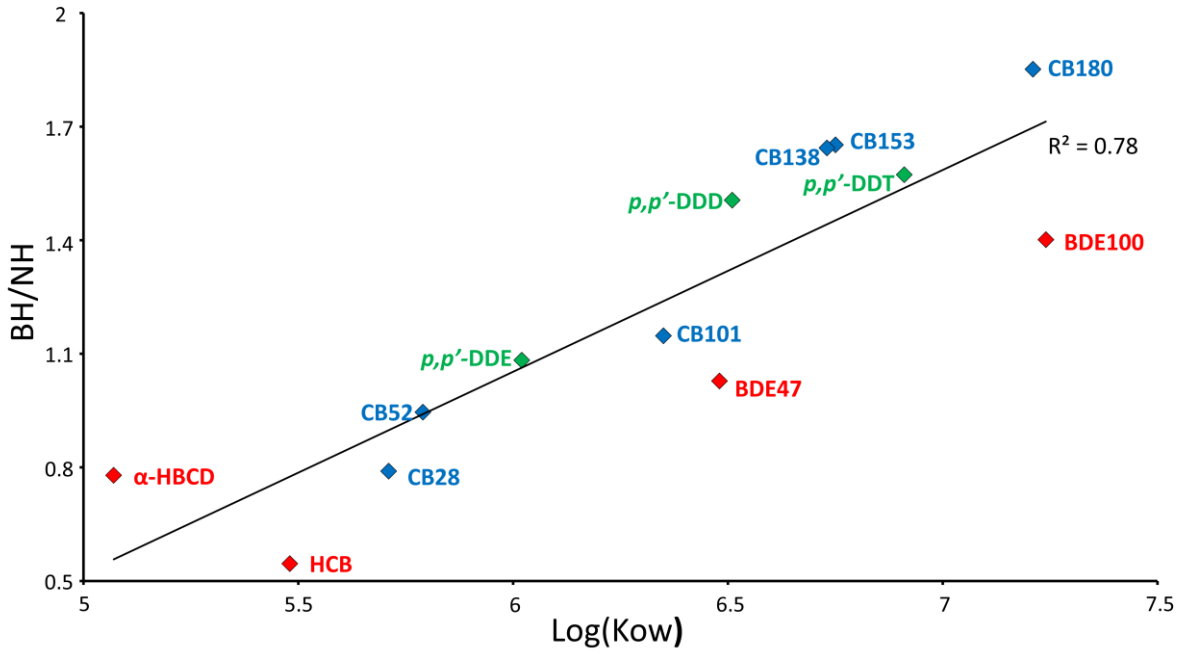


625

626

627

# TABLES

## Table 1: Basic characteristics in narrow-head, intermediate and broad-head eels

| | Mean ± SD | | | ANOVA | | | |
|---|---|---|---|---|---|---|---|
| | **NH** | **INT** | **BH** | ***P*** | $P_{NH\text{-}Int}$ | $P_{Int\text{-}BH}$ | $P_{NH\text{-}BH}$ |
| **Head Width/TotL (-)** | 0.025 ± 0.002 | 0.030 ± 0.002 | 0.035 ± 0.002 | **< 0.01** | **< 0.01** | **< 0.01** | **< 0.01** |
| **Total Length (cm)** | 52.1 ± 3.4 | 53.2 ± 4.9 | 54.5 ± 6.0 | 0.22 | 0.71 | 0.61 | 0.20 |
| **Total Weight (g)** | 224 ± 56 | 253 ± 86 | 273 ± 112 | 0.10 | 0.46 | 0.58 | 0.08 |
| **Age (y)** | 15 ± 3 | 13 ± 2 | 15 ± 3 | **<0.01** | **0.01** | **0.01** | 0.99 |
| **Trophic Position ($\delta^{15}N$, ‰)** | 10.2 ± 1.1 | 11.6 ± 1.8 | 13.0 ± 1.7 | **< 0.01** | **<0.01** | **< 0.01** | **0.01** |
| **Le Cren Condition Factor (-)** | 0.996 ± 0.022 | 1.00 ± 0.02 | 1.00 ± 0.02 | 0.38 | 0.40 | 0.97 | 0.54 |
| **Muscle Fat Content (%)** | 13.4 ± 5.5 | 9.80 ± 4.88 | 8.77 ± 4.88 | **<0.01** | **0.03** | 0.72 | **<0.01** |

SD : Standard Deviation

NH: Narrow-head

INT: Intermediate

BH: Broad-head

**Table 2: Results obtained from the ANCOVA of the different pollutant concentrations between narrow-heads, intermediates and broad-heads. The adjusted means for each group are given, as well as the P-values for slope equality (*P* > 0.05 for ANCOVA) and the *P*-values of the ANCOVA (*P anc*). Significant values are shown in bold.**

| | | TotL (log-transformed) | | | | | | | |
|---|---|---|---|---|---|---|---|---|---|
| | | Adj. Means | | | Slope | | | | |
| | | NH | INT | BH | NH | INT | BH | *P sl eq* | *P anc* |
| Wet Weight/ Lipid Weight (log-transformed) | **Hg** | -1.02 | -0.97 | -0.81 | -1.028 | -0.451 | 0.471 | 0.62 | **< 0.01** |
| | **Zn** | 1.00 | 1.01 | 1.04 | -1.133 | 1.247 | 0.400 | 0.06 | 0.52 |
| | **CB 101** | 2.62 | 2.77 | 2.59 | 1.730 | 0.775 | 0.710 | 0.91 | 0.07 |
| | **CB 153** | 3.12 | 3.29 | 3.30 | 0.179 | 0.978 | 0.719 | 0.93 | **0.01** |
| | **CB 138** | 3.05 | 3.23 | 3.24 | -0.139 | 0.176 | 0.213 | 0.98 | **< 0.01** |
| | **CB 180** | 2.62 | 2.80 | 2.86 | -0.576 | 0.527 | 0.582 | 0.81 | **< 0.01** |
| | **HCB** | 1.08 | 1.00 | 0.85 | 3.030 | -0.092 | 0.731 | 0.26 | **< 0.01** |
| | ***p,p'*-DDE** | 2.45 | 2.60 | 2.58 | 0.380 | -0.007 | 0.300 | 0.97 | **0.03** |
| | **α-HBCD** | 0.99 | 1.03 | 0.81 | -3.444 | -1.017 | -1.394 | 0.73 | 0.08 |
| | **∑PCB** | 3.58 | 3.74 | 3.72 | 0.383 | 0.518 | 0.639 | 0.99 | **0.02** |
| | **∑BDE** | 1.13 | 1.27 | 1.09 | 1.442 | 0.581 | 0.619 | 0.92 | **0.03** |
| | **∑DDT** | 2.53 | 2.68 | 2.64 | 0.597 | -0.062 | 0.285 | 0.94 | 0.05 |
| | | Age (not log-transformed) | | | | | | | |
| | **Hg** | -1.02 | -0.96 | -0.82 | 0.058 | -0.015 | -0.001 | < 0.01 | **< 0.01** |
| | **Zn** | 1 | 1.03 | 1.05 | -0.001 | -0.005 | -0.002 | 0.97 | 0.29 |
| | **CB 101** | 2.62 | 2.79 | 2.64 | -0.044 | 0.009 | 0.021 | 0.10 | 0.18 |
| | **CB 153** | 3.11 | 3.31 | 3.35 | -0.044 | 0.011 | 0.007 | 0.04 | **< 0.01** |
| | **CB 138** | 3.04 | 3.25 | 3.27 | -0.039 | 0.015 | 0.011 | 0.04 | **< 0.01** |
| | **CB 180** | 2.6 | 2.82 | 2.89 | -0.028 | 0.009 | 0.007 | 0.24 | **< 0.01** |
| | **HCB** | 1.07 | 1.01 | 0.85 | 0.003 | 0.018 | 0.023 | 0.77 | **0.01** |
| | ***p,p'*-DDE** | 2.44 | 2.61 | 2.61 | -0.031 | 0.008 | 0.015 | 0.11 | **0.01** |
| | **α-HBCD** | 0.98 | 1.05 | 0.88 | 0.010 | 0.034 | -0.001 | 0.70 | 0.33 |
| | **∑PCB** | 3.57 | 3.75 | 3.76 | -0.039 | 0.013 | 0.011 | 0.05 | **< 0.01** |
| | **∑BDE** | 1.1 | 1.28 | 1.13 | -0.021 | 0.016 | 0.000 | 0.47 | 0.07 |
| | **∑DDT** | 2.52 | 2.69 | 2.67 | -0.033 | 0.008 | 0.016 | 0.08 | **0.02** |

TotL: Total Length

NH: Narrow-head

INT: Intermediate

BH: Broad-head

**Table 3. Results of the non-parametric permutation test (10,000 replicates) performed on the log-transformed pollutant concentrations. Wet weight concentrations were used for metals, lipid weight concentrations for Persistent Organic Pollutants. Significant differences are shown in bold. * indicate pollutants for which the median is presented (as the measured concentrations were not above detection limit in all eels).**

| | | Mean/Median ± SD | | | *P*-values | | |
|---|---|---|---|---|---|---|---|
| | | NH | INT | BH | NH-INT | INT-BH | BH-NH |
| Wet Weight/ Lipid Weight | As | -1.36 ± 0.22 | -1.49 ± 0.42 | -1.55 ± 0.15 | 0.12 | 0.75 | **< 0.01** |
| | Cu | 0.92 ± 0.11 | -0.88 ± 0.14 | -0.77 ± 0.25 | 0.24 | 0.07 | **< 0.01** |
| | Pb | -1.81 ± 0.40 | -1.33 ± 0.66 | -1.55 ± 0.67 | **< 0.01** | 0.26 | 0.10 |
| | Se | -0.84 ± 0.31 | -1.00 ± 0.62 | -1.06 ± 0.63 | 0.26 | 0.72 | 0.10 |
| | Cr* | -1.56 ± 0.49 | -1.57 ± 0.96 | -2.23 ± 0.92 | 0.24 | 0.12 | **< 0.01** |
| | OxC* | 0.40 ± 0.20 | 0.46 ± 0.21 | 0.35 ± 0.26 | 0.37 | 0.07 | 0.24 |
| | TN* | 0.53 ± 0.13 | 0.63 ± 0.18 | 0.54 ± 0.33 | 0.07 | **0.02** | 0.17 |
| | *p,p'*-DDD | 1.70 ± 0.19 | 1.81 ± 0.16 | 1.67 ± 0.33 | **< 0.01** | 0.70 | **0.04** |
| | *p,p'*-DDT* | 0.77 ± 0.20 | 0.88 ± 0.21 | 0.91 ± 0.30 | **< 0.01** | 0.69 | **0.04** |
| | CB 28 | 1.81 ± 0.22 | 1.84 ± 0.19 | 1.53 ± 0.46 | 0.55 | **< 0.01** | **< 0.01** |
| | CB 52 | 2.60 ± 0.20 | 2.68 ± 0.17 | 2.47 ± 0.40 | 0.14 | **0.02** | 0.15 |
| | BDE47 | 0.94 ± 0.21 | 1.09 ± 0.20 | 0.85 ± 0.40 | **0.01** | **< 0.01** | 0.31 |
| | BDE100* | 0.45 ± 0.18 | 0.55 ± 0.21 | 0.58 ± 0.54 | **0.02** | 0.32 | 0.99 |

SD: Standard Deviation

NH: Narrow-head

INT: Intermediate

BH: Broad-head

## SUPPLEMENTARY FIGURES

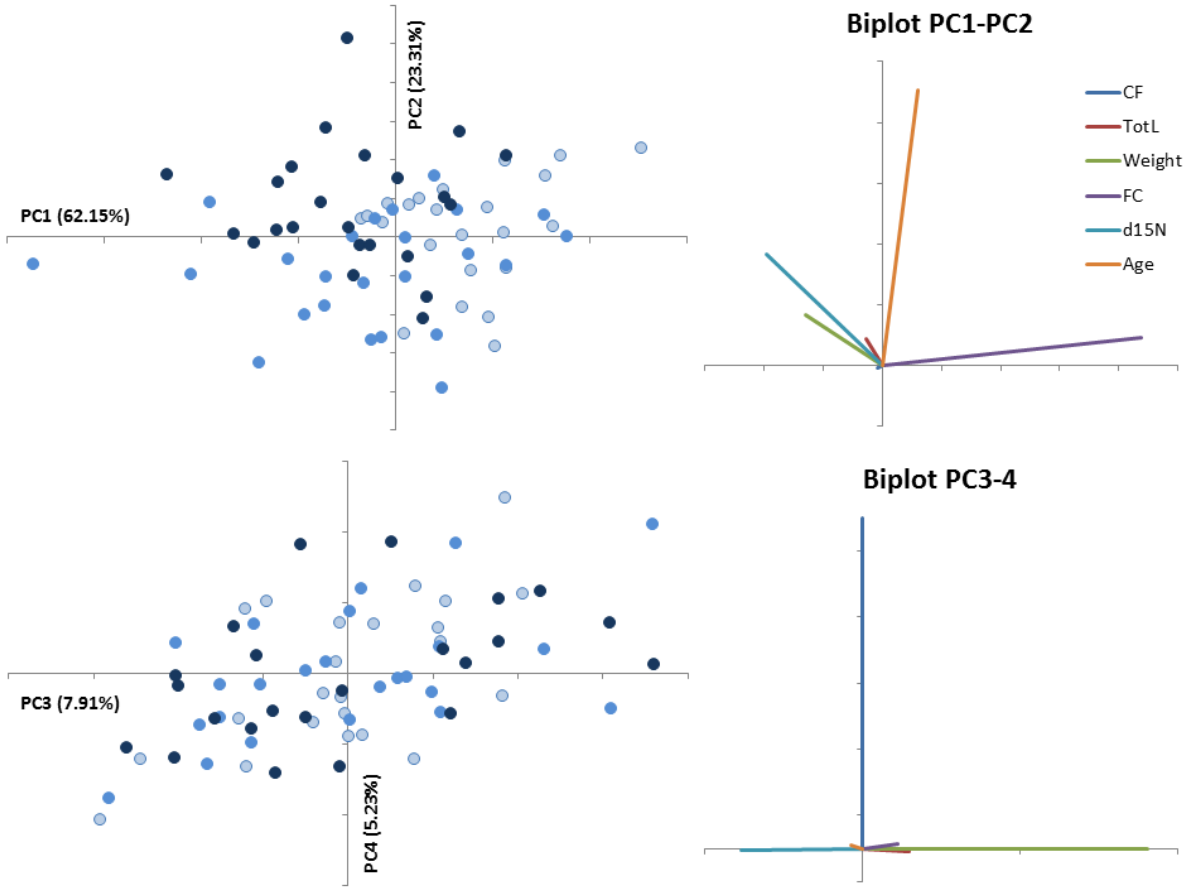


**Fig. S1: Between-group PCA on the different eel measurements and the associated biplot**. The pollutant concentrations were expressed as lipid weight. Light blue dots represents narrow-heads, blue dots intermediates and dark blue dots broad-headed eels. The amount of variation explained by each Principal Component (PC) is shown in parentheses.

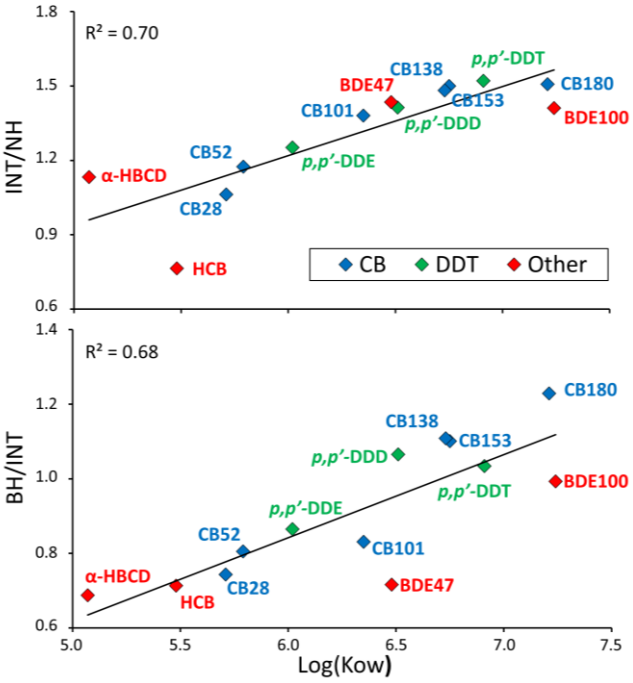


663

664 **Fig. S2: The mean(INT)/mean(NH) and mean(BH)/mean(INT) of the different pollutants**
665 **plotted against the log of their octanol/water partition coefficient (Kow).** The pollutants are
666 expressed as lipid weight. NH: Narrow-heads, INT: Intermediates, BH: Broad-heads. Blue
667 diamonds represent pentachlorobiphenyls (PCBs), green diamonds
668 Dichlorodiphenyltrichloroethanes (DDTs) and red the remaining measured pollutants.

669

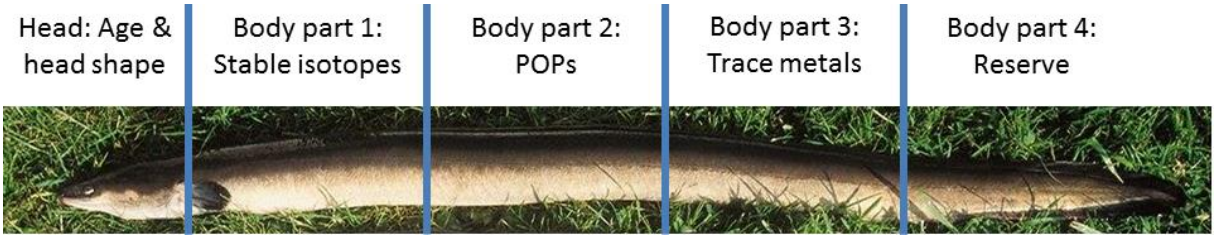


**Fig. S3: The different eel body parts used for the different analyses.**

673 **SUPPLEMENTARY TABLES**

674 **Table S1: The absolute number of specimens for which the pollutant measurement was**
675 **below the detection limit.** The relative number can be found in parentheses (expressed in
676 %). Pollutants that were below the detection limit for more than 50% of the eels were not
677 used for further analyses. NH: Narrow-heads, INT: Intermediates, BH: Broad-heads.

| | NH | INT | BH | TOTAL |
|---|---|---|---|---|
| **CB 28** | 0 (0) | 0 (0) | 0 (0) | 0 (0) |
| **CB 52** | 0 (0) | 0 (0) | 0 (0) | 0 (0) |
| **CB 101** | 0 (0) | 0 (0) | 0 (0) | 0 (0) |
| **CB 138** | 0 (0) | 0 (0) | 0 (0) | 0 (0) |
| **CB 153** | 0 (0) | 0 (0) | 0 (0) | 0 (0) |
| **CB 180** | 0 (0) | 0 (0) | 0 (0) | 0 (0) |
| **OxC** | 5 (19) | 5 (20) | 10 (42) | 20 (27) |
| **TN** | 0 (0) | 1 (4) | 7 (29) | 8 (11) |
| **CN** | 26 (100) | 25 (100) | 24 (100) | **75 (100)** |
| **TC** | 26 (100) | 25 (100) | 24 (100) | **75 (100)** |
| **CC** | 24 (92) | 23 (92) | 23 (96) | **70 (93)** |
| **HCB** | 0 (0) | 0 (0) | 3 (13) | 3 (4) |
| ***p,p'*-DDE** | 0 (0) | 0 (0) | 0 (0) | 0 (0) |
| ***p,p'*-DDD** | 0 (0) | 0 (0) | 0 (0) | 0 (0) |
| ***p,p'*-DDT** | 7 (27) | 2 (8) | 6 (25) | 15 (20) |
| **BDE 28** | 24 (92) | 20 (80) | 21 (88) | **65 (87)** |
| **BDE 47** | 0 (0) | 0 (0) | 0 (0) | 0 (0) |
| **BDE 100** | 0 (0) | 0 (0) | 1 (4) | 1 (1) |
| **BDE 99** | 23 (88) | 25 (100) | 23 (96) | **71 (95)** |

| | | | | |
|---|---|---|---|---|
| **BDE 154** | 18 (69) | 8 (32) | 15 (63) | **41 (55)** |
| **BDE 153** | 19 (73) | 12 (48) | 17 (71) | **48 (64)** |
| **BDE 183** | 26 (100) | 25 (100) | 24 (100) | **75 (100)** |
| **s-DP** | 26 (100) | 25 (100) | 24 (100) | **75 (100)** |
| **a-DP** | 26 (100) | 25 (100) | 22 (92) | **73 (97)** |
| **α-HBCD** | 0 (0) | 0 (0) | 3 (13) | 3 (4) |
| **β-HBCD** | 25 (96) | 24 (96) | 24 (100) | **73 (97)** |
| **γ-HBCD** | 22 (85) | 24 (96) | 24 (100) | **70 (93)** |
| **As** | 0 (0) | 0 (0) | 0 (0) | 0 (0) |
| **Cd** | 25 (96) | 25 (100) | 24 (100) | **74 (99)** |
| **Co** | 15 (58) | 13 (52) | 18 (75) | **46 (61)** |
| **Cr** | 1 (4) | 7 (28) | 9 (38) | 17 (23) |
| **Cu** | 0 (0) | 0 (0) | 0 (0) | 0 (0) |
| **Hg** | 0 (0) | 0 (0) | 0 (0) | 0 (0) |
| **Pb** | 0 (0) | 0 (0) | 0 (0) | 0 (0) |
| **Ni** | 24 (92) | 20 (80) | 18 (75) | **62 (83)** |
| **Se** | 0 (0) | 0 (0) | 0 (0) | 0 (0) |
| **Zn** | 0 (0) | 0 (0) | 0 (0) | 0 (0) |

678

679

**Table S2: Measurements of the different pollutants, expressed as lipid and wet weight.**

The median ± Standard deviation (SD) is given for each phenotype; NH: Narrow-heads, INT: Intermediates, BH: Broad-heads. Also the mean(INT)/mean(NH), mean(BH)/mean(INT) and mean(BH)/mean(NH) ratio of each pollutant is given.

| | | Median ± SD | | | Ratio | | |
|---|---|---|---|---|---|---|---|
| | | NH | INT | BH | INT/NH | BH/INT | BH/NH |
| Lipid weight concentration (ng/ g fat) | **CB 28** | 68.6 ± 27.8 | 72.0 ± 25.4 | 54.0 ± 64.3 | 1.06 | 0.743 | 0.790 |
| | **CB 52** | 413 ± 180 | 480 ± 195 | 415 ± 297 | 1.17 | 0.805 | 0.946 |
| | **CB 101** | 401 ± 285 | 620 ± 300 | 507 ± 405 | 1.38 | 0.831 | 1.15 |
| | **CB 138** | 967 ± 605 | 1,808 ± 782 | 1,926 ± 1,071 | 1.50 | 1.10 | 1.65 |
| | **CB 153** | 1,150 ± 807 | 2,139 ± 966 | 2,336 ± 1,251 | 1.48 | 1.11 | 1.64 |
| | **CB 180** | 381 ± 234 | 721 ± 301 | 771 ± 432 | 1.51 | 1.23 | 1.85 |
| | **Sum PCB** | 3,367 ± 2,013 | 5,626 ± 2,353 | 6,763 ± 3,287 | 1.44 | 1.06 | 1.52 |
| | **HCB** | 11.0 ± 8.6 | 10.4 ± 3.3 | 7.48 ± 4.69 | 0.764 | 0.714 | 0.546 |
| | **α-HBCD** | 10.3 ± 9.2 | 10.4 ± 16.6 | 8.3 ± 9.9 | 1.13 | 0.688 | 0.779 |
| | **TN** | 3.38 ± 1.17 | 4.20 ± 1.46 | 3.43 ± 2.64 | 1.23 | 0.803 | 0.987 |
| | **OxC** | 2.50 ± 0.97 | 2.89 ± 1.13 | 2.25 ± 1.50 | 1.14 | 0.808 | 0.919 |
| | **BDE 47** | 8.99 ± 4.22 | 11.3 ± 7.5 | 11.3 ± 6.9 | 1.43 | 0.716 | 1.03 |
| | **BDE 100** | 2.83 ± 1.35 | 3.56 ± 2.74 | 3.80 ± 3.63 | 1.41 | 0.993 | 1.4 |
| | ***p,p'*-DDE** | 262 ± 122 | 421 ± 152 | 461 ± 244 | 1.41 | 1.07 | 1.51 |
| | ***p,p'*-DDD** | 49.0 ± 24.4 | 67.4 ± 27.1 | 61.3 ± 34.1 | 1.25 | 0.865 | 1.08 |
| | ***p,p'*-DDT** | 5.93 ± 2.27 | 7.49 ± 3.88 | 8.07 ± 5.19 | 1.52 | 1.03 | 1.57 |
| | **Sum DDT** | 312 ± 145 | 485 ± 178 | 529 ± 280 | 1.39 | 1.04 | 1.44 |
| Wet weight concentration (ng/g) | **As** | 0.039 ± 0.039 | 0.037 ± 0.038 | 0.028 ± 0.012 | 0.741 | 0.794 | 0.588 |
| | **Cr** | 0.028 ± 0.025 | 0.027 ± 0.065 | 0.006 ± 0.064 | 1.48 | 0.633 | 0.924 |
| | **Cu** | 0.131 ± 0.029 | 0.131 ± 0.051 | 0.158 ± 0.316 | 1.13 | 1.58 | 1.79 |
| | **Hg** | 0.084 ± 0.064 | 0.095 ± 0.049 | 0.154 ± 0.044 | 1.06 | 1.39 | 1.48 |

| | | | | | | | |
|---|---|---|---|---|---|---|---|
| | **Pb** | 0.013 ± 0.074 | 0.023 ± 0.178 | 0.015 ± 0.156 | 4.30 | 0.743 | 3.20 |
| | **Se** | 0.123 ± 0.411 | 0.103 ± 0.622 | 0.098 ± 0.280 | 1.08 | 0.702 | 0.759 |
| | **Zn** | 9.57 ± 2.6 | 10.4 ± 3.5 | 10.2 ± 2.7 | 1.04 | 1.06 | 1.10 |
| | **CB 28** | 22.8 ± 13.8 | 20.7 ± 14.4 | 9.46 ± 19.7 | - | - | - |
| | **CB 52** | 49.1 ± 26.4 | 41.9 ± 35.9 | 32.7 ± 38.3 | - | - | - |
| | **CB 101** | 47.2 ± 34.1 | 57.9 ± 45.6 | 45.6 ± 46.8 | - | - | - |
| | **CB 138** | 138 ± 89 | 140 ± 113 | 166 ± 102 | - | - | - |
| | **CB 153** | 156 ± 118 | 168 ± 146 | 189 ± 130 | - | - | - |
| | **CB 180** | 53.8 ± 40.1 | 51.0 ± 41.5 | 68.8 ± 36.5 | - | - | - |
| | **Sum PCB** | 445 ± 301 | 497 ± 381 | 493 ± 352 | - | - | - |
| | **HCB** | 1.33 ± 0.80 | 0.86 ± 0.57 | 0.47 ± 0.50 | - | - | - |
| | **α-HBCD** | 1.23± 1.16 | 0.82 ± 2.00 | 0.51 ± 0.543 | - | - | - |
| | **TN** | 0.454 ± 0.170 | 0.347 ± 0.215 | 0.273 ± 0.218 | - | - | - |
| | **OxC** | 0.285 ± 0.149 | 0.248 ± 0.141 | 0.139 ± 0.116 | - | - | - |
| | **BDE 47** | 1.14 ± 0.47 | 0.96 ± 1.65 | 0.58 ± 0.81 | - | - | - |
| | **BDE 100** | 0.367 ± 0.172 | 0.284 ± 0.523 | 0.270 ± 0.300 | - | - | - |
| | ***p,p'*-DDE** | 33.3 ± 20.9 | 32.0 ± 23.8 | 37.5 ± 24.3 | - | - | - |
| | ***p,p'*-DDD** | 5.80 ± 4.53 | 5.09 ± 4.57 | 4.28 ± 3.84 | - | - | - |
| | ***p,p'*-DDT** | 0.60 ± 0.36 | 0.59 ± 0.49 | 0.69 ± 0.42 | - | - | - |
| | **Sum DDT** | 39.6 ± 25.4 | 37.0 ± 28.7 | 42.4 ± 28.3 | - | - | - |

684

685

686 **Table S3: The correlation of the log-transformed wet weight (metals) and lipid weight**

687 **(POPs) concentrations of all specimens (n =75) with total length (TotL) and age.**

| | | TotL | Age |
|---|---|---|---|
| Wet Weight/ Lipid weight (log-transformed) | As | -0.038 | 0.039 |
| | Cr | -0.146 | -0.161 |
| | Cu | 0.062 | 0.203 |
| | Hg | -0.026 | 0.213 |
| | Pb | 0.129 | -0.23 |
| | Se | -0.1 | -0.039 |
| | Zn | 0.118 | -0.068 |
| | CB 28 | 0.149 | -0.055 |
| | CB 52 | 0.144 | -0.054 |
| | CB 101 | 0.133 | -0.12 |
| | CB 153 | 0.139 | -0.15 |
| | CB 138 | 0.064 | -0.11 |
| | CB 180 | 0.096 | -0.08 |
| | OxC | -0.237 | 0.002 |
| | TN | -0.141 | -0.079 |
| | HCB | 0.064 | 0.12 |
| | *p,p'*-DDE | 0.065 | -0.117 |
| | *p,p'*-DDD | 0.117 | -0.119 |
| | *p,p'*-DDT | -0.117 | -0.046 |
| | BDE47 | 0.145 | -0.069 |
| | BDE100 | 0.047 | -0.121 |
| | α-HBCD | -0.189 | 0.04 |

| | | |
|---|---|---|
| ∑PCB | 0.109 | -0.12 |
| ∑BDE | 0.111 | -0.13 |
| ∑DDT | 0.062 | -0.09 |

688

689

690 **Table S4: The P-values of the Shapiro-Wilk test.** Values lower than 0.05 indicate that the data
691 did not fall within a normal distribution. * indicates *P*-values after removal of 1 outlier. Wet
692 weight concentrations were used for the metals, lipid weight concentrations for the Persistent
693 Organic Pollutants**.** NH: Narrow-heads, INT: Intermediates, BH: Broad-heads.

| | | NH | INT | BH | ALL |
|---|---|---|---|---|---|
| Original | TotL | 0.51 | 0.09 | 0.04 | - |
| | Weight | 0.75 | 0.008 | 0.01 | - |
| | Age | 0.09 | 0.2 | 0.41 | - |
| | Muscle Fat content | < 0.01 | 0.47 | 0.07 | - |
| | CF | 0.64 | 0.45 | 0.28 | - |
| | $\delta^{15}N$ | 0.13 | 0.35 | 0.15 | - |
| Log-transformed | Totl | 0.56 | 0.18 | 0.07 | < 0.01 |
| | Weight | 0.96 | 0.06 | 0.30 | 0.08 |
| | Age | 0.04 | 0.07 | 0.19 | 0.15 |
| | Muscle Fat Content | 0.97 | 0.79* | 0.98 | 0.03 |
| Wet Weight/ Lipid weight (log-transformed) | As | < 0.01 | < 0.01 | 0.47 | < 0.01 |
| | Cr | < 0.01 | < 0.01 | < 0.01 | < 0.01 |
| | Cu | 0.02 | 0.03 | < 0.01 | < 0.01 |
| | Hg | 0.26* | 0.75 | 0.28 | < 0.01 |
| | Pb | < 0.01 | < 0.01 | < 0.01 | < 0.01 |
| | Se | < 0.01 | < 0.01 | < 0.01 | < 0.01 |
| | Zn | 0.51 | 0.18 | 0.52 | < 0.01 |
| | CB 28 | 0.85 | 0.82 | 0.03 | < 0.01 |
| | CB 52 | 0.16 | 0.93 | 0.03 | < 0.01 |

| | | | | |
|---|---|---|---|---|
| CB 101 | 0.77 | 0.60 | 0.24 | 0.10 |
| CB 153 | 0.39 | 0.21 | 0.33 | 0.62 |
| CB 138 | 0.22 | 0.29 | 0.30 | 0.65 |
| CB 180 | 0.65 | 0.36 | 0.10 | 0.42 |
| OxC | < 0.01 | < 0.01 | < 0.01 | < 0.01 |
| TN | 0.80 | < 0.01 | 0.01 | < 0.01 |
| HCB | 0.06 | 0.17 | 0.57* | < 0.01 |
| *p.p'*-DDE | 0.30 | 0.76 | 0.07 | 0.43 |
| *p.p'*-DDD | 0.53 | 0.35 | 0.03 | < 0.01 |
| *p.p'*-DDT | < 0.01 | 0.17 | 0.02 | < 0.01 |
| BDE47 | 0.35 | 0.59 | 0.02 | < 0.01 |
| BDE100 | 0.80 | 0.37 | < 0.01 | < 0.01 |
| α-HBCD | 0.73 | 0.10 | 0.19 | 0.23 |
| Sum PCB | 0.22 | 0.24 | 0.09 | 0.48 |
| Sum BDE | 0.79 | 0.40 | 0.18 | 0.27 |
| Sum DDT | 0.51 | 0.61 | 0.06 | 0.27 |

694

695

**Table S5: Results of the sensitivity analysis. The table shows the mean(INT)/mean(NH), mean(INT)/mean(BH) and mean(BH)/mean(NH) ratios for pollutants where concentrations below detection limit were measured and where the non-detects were replaced by the detection limit/2, the minimum concentration (0) and the minimum detection limit.**

| | | DL/2 | Minimum | DL |
|---|---|---|---|---|
| BDE100 | INT/NH | 1.41 | 1.41 | 1.41 |
| | BH/INT | 0.99 | 0.99 | 0.99 |
| | BH/NH | 1.4 | 1.4 | 1.41 |
| HBCD | INT/NH | 1.13 | 1.13 | 1.13 |
| | BH/INT | 0.69 | 0.68 | 0.7 |
| | BH/NH | 0.78 | 0.77 | 0.79 |
| HCB | INT/NH | 0.76 | 0.76 | 0.76 |
| | BH/INT | 0.71 | 0.7 | 0.72 |
| | BH/NH | 0.55 | 0.54 | 0.55 |
| DDT | INT/NH | 1.52 | 1.6 | 1.39 |
| | BH/INT | 1.03 | 1.01 | 1.09 |
| | BH/NH | 1.57 | 1.61 | 1.51 |
| TN | INT/NH | 1.23 | 1.22 | 1.24 |
| | BH/INT | 0.8 | 0.75 | 0.86 |
| | BH/NH | 0.99 | 0.92 | 1.07 |